HEFAT2014
10th International Conference on Heat Transfer, Fluid Mechanics and Thermodynamics
14 – 26 July 2014
Orlando, Florida

EXPERIMENTAL INVESTIGATION OF HEAT TRANSFER FROM A HEATED WALL WITH AN IMPINGING SYNTHETIC JET

Dančová P. *[1,2/], Vít, T.[1,3/] and Sitek P.[1/]
*Author for correspondence
[1/] Dept. of Power Engineering Equipment,
Technical University of Liberec, 46117 Liberec 1, Czech Republic, E-mail: petra.dancova@tul.cz
[2/] Institute of Thermomechanics, CAS, v.v.i.
Dolejškova 5, 180 00 Praha 8, Czech Republic
[3/] IPP CAS (TOPTEC)
Sobotecká 1550, Turnov, Czech Republic, E-mail: vit@ipp.cas.cz

ABSTRACT

This work proposes to investigate a significant advantage of synthetic jets: synthetic jets can be employed successfully to increase heat/mass transfer. The present study is experimental and deals with an investigation into heat transfer from a hot-film probe firmly connected to a wall on which the synthetic jet impinges perpendicularly. All measurements were performed in air by means of thermo-anemometry. The experimental setup consisted of a SJ actuator (emitting orifice diameter, 10 mm), an aluminum flat plate (with dimensions of 120 × 120 mm), and a heated hot-film probe placed on the wall.

INTRODUCTION

A synthetic jet (SJ) is generated by the periodic motion of an actuator oscillating membrane and is synthesized by the interactions within a train of vortex rings or counter-rotating vortex pairs in axisymmetric or two-dimensional geometry; see Smith and Glezer [1]. An impinging synthetic jet offers several noteworthy and ever growing number of applications, one of which is the successful use of a SJ for heat/mass transfer.

The aim of this work is to measure the heat transfer coefficient in air as the working fluid when a SJ impinges perpendicularly on a flat plane. Works by Sholten and Murray [2, 3] were the inspiration for the experimental technique used in this experiment. They employed a hot-film technique to investigate a heated cylinder in a cross air.

In the present paper, the enhancement of heat transfer on the wall by means of SJ impingement was investigated. This problem was also investigated in [4, 5] – specifically, mass transfer was measured using a naphthalene sublimation technique, with the heat transfer evaluated using the heat/mass transfer analogy: The mass transfer data were recalculated into heat transfer as $Nu = Sh \cdot (Pr/Sc)^{0.4}$, where Nu, Sh, Pr, and Sc were the Nusselt, Sherwood, Prandtl, and Schmidt numbers, respectively.

Heat transfer caused by a synthetic jet was investigated, e.g. in [6], in which a passive ducting system designed to reduce the effect of confinement over a range of operating conditions was tested. This work demonstrated that ducted synthetic air jets provided higher rates of heat transfer in confined conditions. This was attributed to the ducting reducing the recirculation of heated air.

Heat and mass transfer in a laminar channel flow equipped with a SJ array was investigated in [7].

NOMENCLATURE

A	[m^2]	Actual probe area
a_h	[1]	Overheat ratio of a probe
D	[m]	Actuator emitting orifice diameter, see Fig. 1
f	[Hz]	Actuating frequency
h	[W/m^{2}K]	Local heat transfer coefficient
H	[m]	Orifice-to-wall spacing, see Fig. 1
L_0	[m]	Extruded fluid column length, $L_0 = U_0 T$
Nu	[1]	Local Nusselt number
Q_{diss}	[W]	Heat released to the surroundings from the probe via convection
R_a	[Ω]	Resistance of probe at ambient temperature T_a
R_{arm}	[Ω]	Resistance of cable and probe holder
R_{senzor}	[Ω]	Resistance of probe
R_{top}	[Ω]	Resistance of the Weatston's bridge branch
Re	[1]	Reynolds number of synthetic jet, $Re = U_0 D/\nu$
SJ		Synthetic jet
St	[1]	Strouhal number of harmonic actuation, $St = D/(\pi L_0)$
t	[s]	Time
T	[s]	Time period
T_a	[K]	Ambient temperature
T_w	[K]	Probe temperature
$u_0(t)$	[m/s]	Orifice velocity
U_0	[m/s]	Time-averaged orifice velocity, $U_0 = f \int_0^{T/2} u_0(t)\, dt$
U	[m/s]	Time-averaged velocity

U_f	[m/s]	Periodic component of the velocity
V_0	[V]	Voltage at the Weatston's bridge without the SJ
V_{forced}	[V]	Voltage on the Weatston's bridge with flow of the SJ

EXPERIMENTAL SETUP AND METHODS

Figure 1 shows the arrangement of the experimental setup, which consisted of a SJ actuator and a flat plate, made from aluminium and measuring 120 × 120 mm. This plate was placed into a wooden frame and firmly conected. Heating foil was attached to the bottom side of the plate. A Dantec 55R47 hot-film probe was placed in the middle of the plate's upper side. The actual area of the heated element was 0.1 × 0.9 mm. The probe was connected to a Dantec 90C10 anemometer in constant temperature mode.

A Dantec 55P11 hot-wire probe and the same Dantec 90C10 anemometer were used (again, in constant temperature mode) to measure orifice velocity.

The SJ actuator consisted of a sealed cavity with an emitting orifice (diameter D = 10 mm) and two TVM ARN-100-10/4 loudspeakers – see Figure 1. The SJ actuator was placed on a traverser, which enabled movement in all three directions along the Cartesian coordinate system.

The SJ actuator was fed with a sinusoidal signal from a Tektronik AFG 2102 signal generator and amplified by an Omnitronic MPZ180 amplifier; both actuator loudspeakers were connected in parallel.

A type-K thermocouple was placed on both sides of the plate to monitor wall temperature.

To evaluate the heat transfer coefficient (h), the hot-film probe operated in conjunction with a constant temperature anemometer as a resistor in one arm of the Wheatston's bridge. To evaluate convective heat transfer in relation to the impinging SJ, measurements were taken in two regimes, with and without the SJ in operation. Based on the results of those experiments, taking into account the material properties of the probe used, and using the standard correlations for convective heat transfer calculation, the heat released to the surroundings by convection was evaluated as, [3, 13]:

$$Q_{diss} = \left(V_{\text{forced}}^2 - V_0^2\right) \frac{R_{\text{senzor}}}{\left(R_{\text{arm}} + R_{\text{top}}\right)^2}, \qquad (1)$$

where V_{forced} was the voltage on the bridge with the SJ flow, V_0 the voltage on the bridge without the SJ, R_{senzor} the constant resistance dependent on the probe overheat ratio, R_{arm} the resistance of the cable and probe holder, and R_{top} the resistance of the Weatston's bridge branch where the probe was also connected.

The resulting heat transfer coefficient h was obtained when Q_{diss} was divided by the difference between temperature of the probe and of the flowing medium and by the effective area of the probe. From this, and by rearranging Newton's cooling law, h can be calculated as:

$$h = \frac{Q_{\text{diss}}}{A_{\text{eff}}(T_{\text{w}} - T_{\text{a}})}, \qquad (2)$$

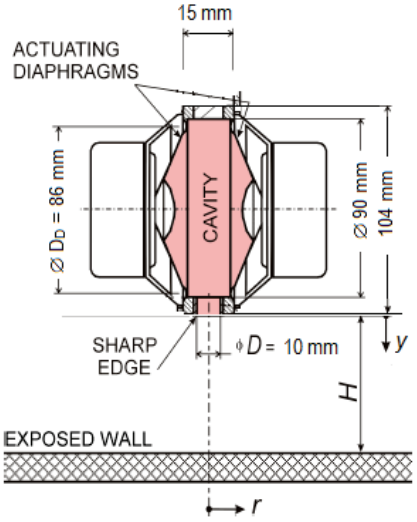

(a)

(b)

Figure 1 (a) Synthetic jet actuator design, by Trávníček et *al.* [4], (b) real situation of the experiment

where T_w and T_a are probe and ambient temperature respectively, A_{eff} is the effective area of the probe, which is estimated as A_{eff} = 1.5 A, according to [8], where A is the actual heated element area. A_{eff} takes lateral conduction into the plate into account, [8].

RESULTS

Two signals were recorded during heat transfer and the velocity experiments – one signal from the anemometer and an auxiliary rectangular signal from the signal generator. The rectangular signal levels were 3.4 V and 0.1 V; the value of 3.4 V corresponds to the SJ exhaust stroke and the value 0.1 V to the SJ suction stroke. A phase averaging of the anemometer signal was made based on the auxiliary signal.

Nominal frequency of the SJ actuator

Experiments were performed over a frequency range of 30-300 Hz, with a power supply of 3 W.

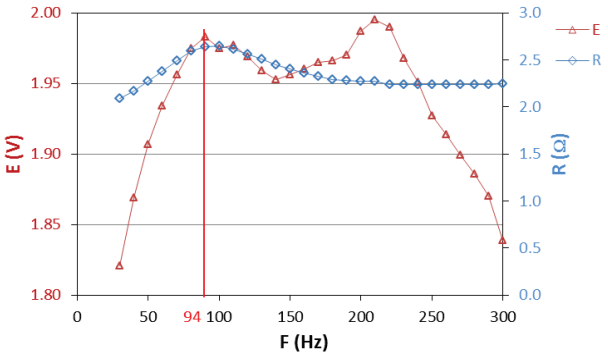

Figure 2 SJ actuator frequency characteristic

It is a known fact that the natural frequencies of loudspeaker-based actuators can be estimated from their impedances [9]. Figure 2 shows the measured impedance (R) and the hot-wire anemometer voltage output (E). Both curves clearly indicate the first resonance of the SJ actuator to be 94 Hz. Therefore, 94 Hz was chosen as the nominal frequency for the present experiments.

Velocity measurement

An experimental evaluation of orifice velocity was made at frequencies of 30, 40, 50, and 94 Hz. The actuator was fed with a sinusoidal current with 3 W of power. The sampling frequency and the number of samples were 64 kHz and 32,768, respectively. From the velocity experiments, the time-averaged orifice velocity was determined and the Reynolds number evaluated (see Table 1):

Table 1 Dependence of time-averaged orifice velocity and Reynolds number on actuating frequency

f (Hz)	U_0 (m/s)	Re
30	4.82	3187
40	6.44	4263
50	7.82	5170
94	10.92	7226

Kinematic viscosity (ν = 15.116·10^{-6} m^2/s) was used to calculate the Reynolds number.

Figure 3 demonstrates the dependence of the time-mean velocity (in dimensionless form) on the y axis (i.e. axis of the actuator orifice, see Figure 1) in the logarithmic scale for frequencies of 40 and 94 Hz. The slope of the line relating to the two regions of the SJ is visible. The exponents of velocity decay $U \sim y^n$ were n = (−0.419 - −0.435) and n = (−1.035 - −1.023), respectively. A similar behavior was also observed in [5, 10], where n = -0.43 and n = -1.04. In all cases, the exponents were the same or very similar. This indicates that they were not influenced by SJ actuator design, by the working fluid, or by the working frequency. Exponent n = (−1.035 - −1.023) confirms that a SJ in the distant field has the character of a continual fluid jet. It is a well-known fact that the stream-wise velocity decay of conventional (steady), axisymmetric and fully-developed turbulent jets is $U/U_0 \sim (y/D)^{-1.0}$; see Schlichting and Gersten, [11].

Heat transfer

Heat transfer experiments were performed for three different overheat ratios of the probe (0.10, 0.16, and 0.24) at distances from the actuator orifice of y/D = 1, 2, 4, 6, and 10. The overheat ratio a_h of the probes working in a thermo-anemometry constant temperature mode was used as a reference for adjusting probe temperature, [12]. It can be calculated as $a_h = {R_{sensor}}/{R_a}$, where R_a is the resistance of the probe at ambient temperature. Probe temperatures, depending on the overheat ratios, were 28.57, 45.72, and 68.57 °C. The temperature of the wall was kept at the same value as the ambient temperature, i.e. 24 °C. The SJ actuator was fed with a sinusoidal signal with a frequency of 30, 40, and 50 Hz and with a power output of 3 W. These frequencies, which fall below the nominal 94 Hz, were chosen due to the rather slow capture speed of the probe. The sampling frequency was set at 10 kHz, and the number of samples was set at 4,096.

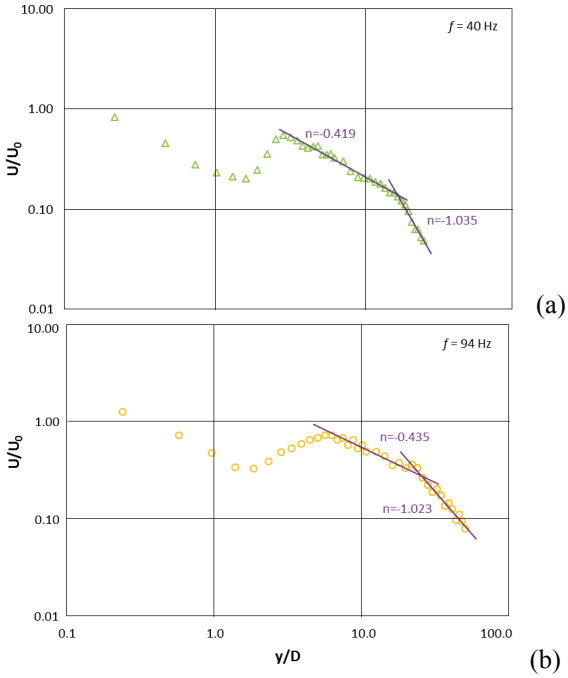

Figure 3 Dependence of the time-mean velocity on the distance from the orifice in a logarithmic scale
(a) f = 40 Hz, (b) f = 94 Hz

Figures 4 and 5 show the principle of evaluation of h. Measurements were carried out for three defined overheat ratios, i.e. three types of experiments at every point. Data received from the probe were recalculated to Q_{diss} using eq. (1). The heat transfer coefficient for each set overheat ratio was evaluated using eq. (2), see Figure 4. Figure 5 shows measurement at one position (e.g. r/D = 1) for three probe overheat ratios. From these points, the resulting heat transfer

coefficient was calculated as $h = A \cdot \ln(x) + B$, where A and B were constants changed for every position of r/D. Resulting heat transfer coefficient was calculated assuming $x = T_w/T_a = 1$, [14].

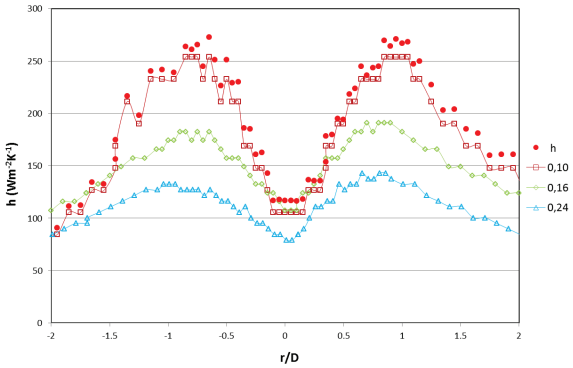

Figure 4 The resulting heat transfer coefficient (h) and heat transfer coefficient measured with different probe overheat ratios (0.10, 0.16, and 0.24)

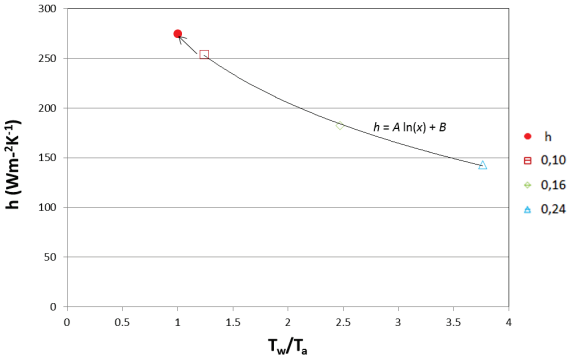

Figure 5 Evaluation of the resulting heat transfer coefficient at $r/D = 1$

Figure 6 shows the radial distribution of the heat transfer coefficient h at a frequency of 50 Hz. As the distance increases, the h value decreases. Nevertheless, the h influence is also seen at a distance of 10 diameters distant from the actuator orifice. Distribution of h is symmetric. From the orifice axis $r/D = 0$, the value of h increases to its maximum – the first peak. At distance r/D from 1.4 to 1.7, the secondary peak is visible (marked in Figure 7). Figure 7 shows h distribution on the wall (r/D) for different distances from the actuator orifice to the wall $y/D = 2$ (right side) and $y/D = 4$ (left side). According to experiments using the Dantec 55R47 hot-film probe, the highest values of h were achieved at a frequency of 50 Hz. However, the highest value is assumed to be at the natural frequency of 94 Hz.

CONCLUSIONS

This work measured the heat transfer coefficient on a wall, which was cooled by an impacted SJ. Wall temperature was maintained at 24 °C, the same as the ambient temperature. A heated, glue-on film probe was placed on the wall.

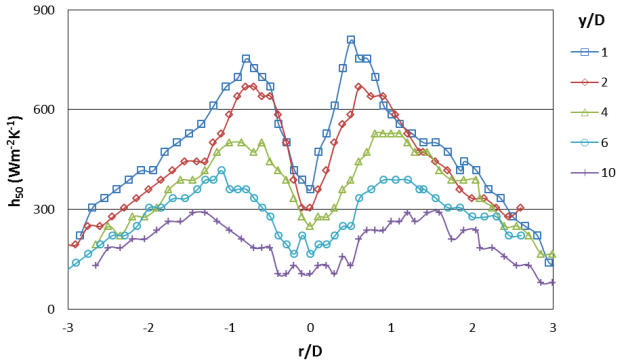

Figure 6 Heat transfer coefficient distributions for frequency 50 Hz at different distances

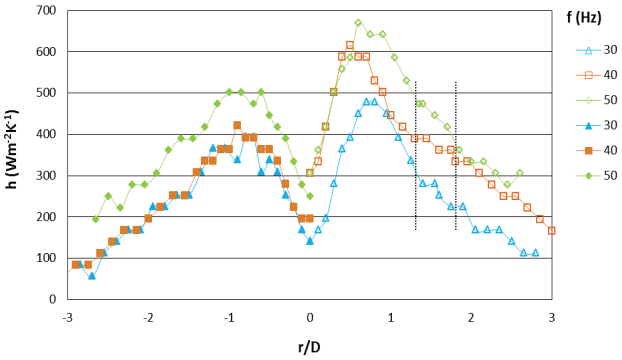

Figure 7 Heat transfer coefficient distribution for different frequencies at distance $y/D = 2$ (right side) and $y/D = 4$ (left side)

The nominal frequency of 94 Hz was chosen at the first resonance. Due to the capture speed of the probe, h was investigated at frequencies lower than the nominal frequency. Experiments were performed at 30, 40, and 50 Hz. The value of h was obtained from the ratio of convective heat, the temperature difference, and the effective probe area. h was measured in a range of 30-850 $Wm^{-2}K^{-1}$ and the highest value was identified at a distance of 1 diameter from the SJ actuator orifice and at a frequency of 50 Hz.

Velocity measurement was used to obtain the time-averaged orifice velocity and Reynolds number. The measurement was carried out at different frequencies (30, 40, 50, and 94 Hz).

During velocity experiments in vicinity of the SJ actuator orifice, the mean time orifice velocity was estimated as 4.82, 6.44, 7.82, and 10.92 m/s at frequencies of 30, 40, 50, and 94 Hz. SJ velocity along the y axis of the actuator orifice was also measured. Results from these experiments confirm that the behavior of the SJ is independent of the design of SJ actuator, the working fluid, and the working frequency.

This work will continue to measure h with different experimental methods. Results from this work will be used to

fine tune experimental device settings and measurement conditions.

Acknowledgements
We gratefully acknowledge the support of the CR Grant Agency (project No. 14-08888S), the ESF operational program "Education for Competitiveness" in the Czech Republic in the framework of project "Support of engineering of excellent research and development teams at the Technical University of Liberec" No. CZ.1.07/2.3.00/30.0065. We would also like to thank project SGS 21000.

REFERENCES

[1] Smith, B.L., and Glezer, A., The formation and evolution of synthetic jets, *Phys. Fluids*, Vol. 10, 1998, pp. 2281-2297
[2] Scholten J.W., and Murray, D.B., Measurement of convective heat transfer using hot film sensors: correction for sensor overhear, *Transaction of the ASME - J. of Heat Transfer*, Vol. 118, 1996, pp. 982-984
[3] Scholten, J.W., and Murray, D.B., Unsteady heat transfer and velocity of a cylinder in crossflow – I. Low freestream turbulence, *Int. J. Heat Mass Transfer*, Vol. 41, No. 10, 1998, pp. 1139-1148
[4] Trávníček, Z., and Tesař, V., Annular synthetic jet used for impinging flow mass–transfer. *Int. J. Heat Mass Transfer*, Vol. 46, 2003, pp. 3291–3297
[5] Trávníček, Z., Vogel, J., Vít, T., and Maršík, F., Flow field and mass transfer experimental and numerical studies of a synthetic impinging jet, *4th international conference HEFAT 2005*, Cairo, Egypt, 2005, paper number ZT4
[6] Rylatt, D., O' Donovan, T.S., Heat transfer to a ducted, semi-confined impinging synthetic air jet, *14th International Heat Transfer Conference* (*IHTC14*), Washington DC, 2010
[7] Trávníček, Z., Dančová, P., Kordík, J., Vít, T., Pavelka, M., Heat and mass transfer caused by a laminar channel flow equipped with a synthetic jet array. *Trans. ASME, J. Thermal Science and Engineering Applications* 2, 2010, 041006
[8] Beasley, D.E., Figliola, R.S., A generalized analysis of a local heat flux probe, *J. Physics E-Scientific Instruments.*, Vol. 21, 1988, pp. 316-322
[9] Persoons, T., General reduced-order model to design and operate synthetic jet actuators, *AIAA Journal*, Vol. 50, 2012, pp. 916-927
[10] Trávníček, Z., Vít, T., de Boer, P., Maršík, F., Synthetic jets – design and verification of the actuato, *Conference Topical Problems of Fluid Mechanics 2004*, Prague, Czech Republic, 2004, pp. 165-168
[11] Schlichting, H., Gersten, K., *Boundary-Layer Theory*. Springer-Verlag, Berlin, 2000
[12] Bruun, H.H., *Hot wire anemometry*, Oxford Univ. Press, 1995
[13] http://www-g.eng.cam.ac.uk/whittle/current-research/hph/hot-film/hot-film.html (cited 3.2.2014)
[14] Sitek, P., *Measuring of heat transfer coefficient using hot wire anemometry*, Bachelor's thesis, Technical University of Liberec, 2013
[15] Dančová, P., Vít, T., Trávníček, Z., Lédl, V., Measurement of temperature fields in fluids, *7th International Symposium on Turbulence, Heat and Mass Transfer*, Palermo, Italy, 2012
[16] Trávníček, Z., Dančová, P., Vít, T., Visualization and heat/mass transfer study of laminar channel flow controlled by synthetic jet array, *The 7th Pacific Symposium on Flow Visualization and Image Processing*, Nov. 16-19, 2009 Kaohsiung, Taiwan, R.O.C, 2009.
[17] Dančová, P., Vít, T., Analysis of the Synthetic Jet, *Journal of Applied Science in the Thermodynamics and Fluid Mechanics* (*JASTFM*), 1st issue 2008, 2008 (web version)
[18] Garg, J., Arik, M., Weaver, S., Wetzel, T., Saddoughi, S., Advanced localized air cooling with synthetic jets, *ASME Journal of Electronics Packaging* 127, 2005, pp. 503–511
[19] Scholten, J.W., and Murray, D.B., Unsteady heat transfer and velocity of a cylinder in crossflow – II. High freestream turbulence, *Int. J. Heat Mass Transfer*, Vol. 41, No. 10, 1998, pp. 1149-1156
[20] Timchenko, V., Reises, J., Leonardi, E., Heat transfer enhancement in micro-channels by synthetic jets, *4th International Conference on Computational Heat and Mass Transfer*, Paris-Cachan, May 17-20, 2005, pp. 471-476